2017 American Control Conference
Sheraton Seattle Hotel
May 24–26, 2017, Seattle, USA

Optimal Energy Storage Control for Frequency Regulation under Temporal Logic Specifications

Zhe Xu, Agung Julius and Joe H. Chow

Abstract— **A formal safety controller synthesis method for power grid frequency regulation using energy storage systems is proposed. After a fault, with uncertainties in the fault clearing time, the generator machine angles and rotor speed deviations will enter a set of post-fault states that can be over-approximated using reachability analysis. We use the robust neighbourhood approach to cover this set using the initial robust neighbourhood of finitely many simulated post-fault trajectories. We design these simulated trajectories to meet the frequency regulation requirements specified in Metric Temporal Logic (MTL) by optimizing the input signals through a functional gradient descent approach. In this way, all the possible post-fault trajectories with the given uncertainties in the fault clearing time are guaranteed to satisfy the MTL specification. Further, a piecewise linear control law is learned from the data of the simulated trajectories to generate a feedback controller that is more reactive to unexpected disturbances.**

I. Introduction

With the increasing incorporation of renewable energy in the ancillary services, modern power systems are utilizing diversified power resources for providing more reliable and efficient services. Energy storage systems such as spinning reserves and battery energy storage systems serve as buffers of the power system to restore grid frequency to the allowable range [1]. As different services and storage systems have different response time and duration time, the regulated frequency could have different temporal properties. Therefore, temporal logics [2], [3], [4] can be utilized to provide time-related specifications such as “after a fault is cleared, the grid frequency should be restored to 60Hz±0.2Hz within 2 seconds and to 60Hz±0.02Hz within 20 seconds”. There are a lot of literature on the control of energy storage systems for economic and stability benefits, while incorporating temporal logic constraints into the controller synthesis problem is still a novel approach.

Currently, there are two main categories of approaches in designing controllers that meet certain temporal logic specifications. The first category of approaches abstract the system as a transition system and transform the controller synthesis problem into a series of constrained reachability problems [5], [6], [7]. The second category of approaches convert the controller synthesis problem into a single optimal control problem and encode the temporal logic specifications as optimization constraints on the optimization variables. For the optimization problem formulation, some authors formulate it as a Mixed-Integer Linear Programming (MILP) problem for Mixed Logical Dynamical (MLD) systems [8], [9] while some other authors substitute the temporal logic constraint into the optimization objectives and apply a functional gradient descent algorithm on the resulting unconstrained problem. In [10], the authors propose an optimal safety controller synthesis method for continuous nonlinear systems using functional gradient descent. In [11], the authors apply the method in the falsification of Metric Temporal Logic (MTL) specifications and the controller synthesis can be achieved by falsifying the negation of the MTL formulae. In [12], the authors replace the feedforward controller obtained in [10] with a feedback controller and a piecewise linear control law is learned from the data of the simulated trajectories following the approach of [13].

In this paper, we modify the functional gradient descent method in [11] and the feedback control law generation method in [12] to regulate grid frequencies utilizing energy storage systems. We seek the minimal-storage-effort control to satisfy certain MTL specifications of the frequency deviations and machine angles. Different from [11], we formulate the MTL specification as a constraint and we apply the functional gradient descent method to both satisfy the MTL constraint and minimize the storage control effort. The power system nonlinear dynamics is first feedback linearized and the obtained linear system has a control autobisimulation function which can bound the trajectories that start from an initial set within the robust neighbourhood [14]. We simulate finitely many post-fault trajectories with different fault clearing time such that the initial robust neighbourhood of these simulated trajectories can cover the over-approximated reachable set of the post-fault states with given uncertainties in the fault clearing time. Then we compute the optimal storage control input signals for the post-fault trajectories through the functional gradient descent method. Further, we generate a feedback controller by identifying a piecewise linear control law from the data of the optimal input signals and the states of the simulated trajectories. Different from other works, we use robust linear programming to find the classification functions for the subclasses and construct piecewise linear classifiers in partitioning the state space.

This paper is structured as follows. Section II reviews the control autobisimulation function and shows the controller synthesis methods for both the feedforward and feedback controllers. Section III shows the implementation of the algorithms on a double-machine infinite-bus power system model to control the energy storage systems for power system frequency regulation under Temporal Logic specifications. Finally, some conclusions are presented in Section IV.

Zhe Xu, Agung Julius and Joe H. Chow are with the Department of Electrical, Computer, and Systems Engineering, Rensselaer Polytechnic Institute, Troy, NY 12180, USA e-mail: xuz8, juliua2, chowj@rpi.edu.

978-1-5090-5992-8/$31.00 ©2017 AACC

II. Controller Synthesis

A. Control Autobisimulation Function

Consider a nonlinear dynamical system with input

$$\dot{x} = F(x, u), \tag{1}$$

where $F : \mathbb{R}^n \times \mathbb{R}^m \to \mathbb{R}^n$ and $u \in L^2[0, T]$.

The concept of the control autobisimulation function (CAF) is described in [14]. For nonlinear system dynamics that is feedback linearizable (such as the power system dynamics in Sec. III), we can introduce a new control input $\omega(\tau)$ and design a feedback law $u = \kappa(x) + \lambda(x)\omega$ to make the closed-loop system with the new input ω as a linear system, as shown in Fig. 1. We denote the feedback linearized system dynamics as $\dot{z} = Az + B\omega$, where z is the new state of the feedback linearized system. Then we can design another input signal v such that $\omega = Kz + v$, where K is chosen such that $A + BK$ is Hurwitz. For the obtained stable linear system $\dot{z} = (A + BK)z + Bv$, a control autobisimulation function can be formed as $\psi(z, z') = \sqrt{(z - z')^T P(z - z')}$, where P can be calculated by the following Linear Matrix Inequalities:

$$\begin{gathered} P^T = P \succeq 0, \\ (A + BK)^T P + P(A + BK) \preceq 0. \end{gathered} \tag{2}$$

For brevity, we denote $f(z, v) = (A + BK)z + Bv$. We denote the solution of $\dot{z} = f(z, v)$ as $\xi(\tau; z_0, v)$ where $z_0 = z(0)$ is the initial state of the feedback linearized system. Using the inverse mapping of $z(x)$, we have $x = z^{-1}(\xi(\tau; z_0, v))$. We denote $B_\psi(z, r) \triangleq \{z' | \psi(z, z') \leq r\}$ as the robust neighbourhood of a point z in the shape of an ellipsoid (robustness ellipsoid) and r is referred to as the radius of the ellipsoid. As the control autobisimulation function is non-increasing through time, it is guaranteed that for any initial state $z'_0 \in \mathbb{R}^n$ and any control signal $v(\tau)$, if the initial distance $\psi(z_0, z'_0) = \gamma$, then for any time τ, $\xi(\tau; z'_0, v) \in B_\psi(\xi(\tau; z_0, v), \gamma)$.

B. Feedforward Controller Synthesis

The feedforward controller synthesis problem is to find the input v such that the trajectory $\xi(\tau; z_0, v)$ satisfies the MTL specification ϕ with minimal control efforts. The syntax and semantics of the Metric Temporal Logic are described in [15]. The optimization problem is formulated as follows:

$$\begin{aligned} \text{min.} & \int_0^T g(\xi(\tau; z_0, v), v(\tau)) d\tau \\ \text{s.t.} \quad & [[\phi]]\, (\xi(\tau; z_0, v), 0) \geq \zeta, \end{aligned} \tag{3}$$

where ζ is a positive number to avoid too small robustness ellipsoid, $[[\phi]]\, (\xi(\tau; z_0, v), 0)$ is the robustness degree (for the definition of robustness degree, see [15]) of the trajectory $\xi(\tau; z_0, v)$ with respect to the formula ϕ at time 0 and $g(\xi(\tau; z_0, v), v(\tau))$ can be expressed as follows:

$$\begin{aligned} g(\xi(\tau; z_0, v), v(\tau)) = \|u(\tau)\|^2 = || \Big(& \kappa\big(z^{-1}(\xi(\tau; z_0, v))\big) \\ & + \lambda\big(z^{-1}(\xi(\tau; z_0, v))\big)\big(K\xi(\tau; z_0, v) + v(\tau)\big)\Big) ||^2. \end{aligned}$$

We denote the domain of the state z as $\mathbb{X}$, the distance from z to a set S as $\mathbf{dist}_d(z, S) \triangleq \inf\{d(z, y) | y \in cl(S)\}$, where d is a metric on $\mathbb{X}$ and $cl(S)$ denotes the closure of the set S. We denote the set of states that satisfy the atomic proposition π as $\mathcal{O}(\pi)$, the depth of z in S as $\mathbf{depth}_d(z, S) \triangleq \mathbf{dist}_d(z, \mathbb{X} \setminus S)$, the signed distance from x to S as

$$\mathbf{Dist}_d(z, S) \triangleq \begin{cases} -\mathbf{dist}_d(z, S) & \text{if } z \notin S; \\ \mathbf{depth}_d(z, S) & \text{if } z \in S. \end{cases} \tag{4}$$

We can use functional gradient descent method to decrease $[[\neg\phi]]\, (\xi(\tau; z_0, v), 0)$ at each iteration step until the constraint is satisfied. According to Proposition 3.1 in [16], for the MTL formula $\neg\phi$, there exists a critical time $\tau_r \in [0, T]$ and a critical proposition π_r that appears in ϕ such that $[[\neg\phi]]\, (\xi(\tau; z_0, v), 0) = \mathbf{Dist}_d(\xi(\tau_r; z_0, v), \mathcal{O}(\pi_r))$. Thus the robustness degree of the trajectory $\xi(\tau; z_0, v)$ with respect to $\neg\phi$ can be calculated by identifying the critical time τ_r and the critical proposition π_r (which can be easily computed using software such as S-TaLiRo [17]).

Thus at each iteration the optimization problem is converted to the following problem:

$$\begin{aligned} \text{min.} & \int_0^T g(\xi(\tau; z_0, v), v(\tau)) d\tau \\ \text{s.t.} \quad & G(\xi(\tau_r; z_0, v)) + \zeta \leq 0, \end{aligned} \tag{5}$$

where $G(\xi(\tau_r; z_0, v)) = \mathbf{Dist}_d(\xi(\tau_r; z_0, v), \mathcal{O}(\pi_r))$. In the following, we denote $J(v) \triangleq \int_0^T g(\xi(\tau; z_0, v), v(\tau)) d\tau$ and $J_{con}(v) \triangleq G(\xi(\tau_r; z_0, v)) + \zeta$ as the objective function and the constraint function respectively.

We compute the functional derivative of $J(v)$ for the input $v(\tau)$ in the direction $\hat{v}$,

$$dJ(v; \hat{v}) \triangleq \lim_{\delta \to 0} \frac{J(v + \delta\hat{v}) - J(v)}{\delta}. \tag{6}$$

If we denote $q(\cdot)$ as the gradient of J in the function space of $v(\cdot)$, then we have

$$dJ(v; \hat{v}) \triangleq \langle q, \hat{v} \rangle = \int_0^T q(\tau)\hat{v}(\tau) d\tau. \tag{7}$$

Similarly, the functional derivative of $J_{con}(v)$ for the input $v(\tau)$ in the direction $\hat{v}_{con}$ can be written as follows:

$$\begin{aligned} dJ_{con}(v; \hat{v}_{con}) & \triangleq \lim_{\delta \to 0} \frac{J_{con}(v + \delta\hat{v}_{con}) - J_{con}(v)}{\delta} \\ & \triangleq \langle q_{con}, \hat{v}_{con} \rangle = \int_0^T q_{con}(\tau)\hat{v}_{con}(\tau) d\tau. \end{aligned} \tag{8}$$

where $q_{con}(\cdot)$ is the gradient of J_{con} in the function space of $v_{con}(\cdot)$.

We use the following notations for the sake of brevity:

$$\begin{gathered} \frac{\partial G(\tau_r)}{\partial z} \triangleq \frac{\partial G}{\partial z} |_{\xi(\tau_r; z_0, v)} \\ \frac{\partial f(\tau)}{\partial z} \triangleq \frac{\partial f}{\partial z} |_{(\xi(\tau; z_0, v), v(\tau))}, \quad \frac{\partial f(\tau)}{\partial v} \triangleq \frac{\partial f}{\partial v} |_{(\xi(\tau; z_0, v), v(\tau))}, \\ \frac{\partial g(\tau)}{\partial z} \triangleq \frac{\partial g}{\partial z} |_{(\xi(\tau; z_0, v), v(\tau))}, \quad \frac{\partial g(\tau)}{\partial v} \triangleq \frac{\partial g}{\partial v} |_{(\xi(\tau; z_0, v), v(\tau))} . \end{gathered} \tag{9}$$

Following similar mathematical deductions with those in [10], it can be calculated that the gradients $q(t) = \frac{\partial g(t)}{\partial v} + \int_t^T \frac{\partial g(\tau)}{\partial z} p_\tau(t) d\tau$, $q_{con}(t) = \frac{\partial G(\tau_r)}{\partial z} p_{\tau_r}(t)$, where $p_\tau(t) = \int_t^\tau \frac{\partial f(s)}{\partial z} p_s(t) ds + \frac{\partial f(t)}{\partial v}$ is an $\mathbb{R}^{n \times m}$-valued function which is specified to be zero if $\tau < t$. To make the computation easier to handle, we specify the input signal $v(\tau)$ to be a piecewise constant function of time, i.e $v(\tau) = v[k]$ for $kT_s \leq \tau \leq (k+1)T_s$ where T_s is a sampling period. Then $p_\tau(t)$ can be computed as state trajectories of the following Linear Time Invariant (LTI) system:

$$\frac{dp_\tau(t)}{d\tau} = \frac{\partial f(\tau)}{\partial z} p_\tau(t) = (A + BK) p_\tau(t) \tag{10}$$

with the initial condition $p_t(t) = \frac{\partial f(t)}{\partial v} = B$ at $t = kT_s (k = 0, 1, \ldots, N)$. Then $p_{\tau_r}(t)$ can be calculated by taking the value of $p_\tau(t)$ when $\tau = \tau_r$. Thus $q(t)$ and $q_{con}(t)$ can be calculated at $t = kT_s$ $(k = 0, 1, \ldots, N)$.

After $q(kT_s)$ and $q_{con}(kT_s)$ are computed, we specify $q(\tau) = q(kT_s)$ and $q_{con}(\tau) = q_{con}(kT_s)$ for $kT_s \leq \tau \leq (k+1)T_s$. Our functional gradient descent algorithm is similar to the algorithm in [11] and [10], but we consider the constraint function while minimizing the objective function. If the current solution satisfies the constraint, then the next solution will be optimized along the opposite direction of the gradient of the objective function; otherwise, the next solution will be optimized along the opposite direction of the gradient of the constraint function as the constraint has to be met before the objective function is further minimized.

C. Feedback Controller Synthesis

In this section, we generate a feedback control law using system identification techniques to replace the open-loop input signals of the feedforward controller. The advantage of a feedback controller is that it is more reactive to unexpected disturbances and the required memory is reduced from storing many signals to only a set of piecewise linear control laws [12]. When the states and inputs of the trajectories are calculated using numeric simulators such as ODE or CVODE, the data are discrete and therefore in the following we use $\xi(k; z_0, v)$ to denote the flow solution $\xi(t; z_0, v)$ at the kth time instant.

Theorem 1 ([12]): Suppose that $\|\epsilon\|_\infty \leq \delta$, then there exists a critical radius $\gamma_{crit} > 0$ such that for any $\gamma > \gamma_{crit}$ the following is true for all $k > 0$:
$\psi(z_0, z_0') \leq \gamma \Rightarrow \psi(\xi(k; z_0, v), \xi(k; z_0', v + \epsilon)) \leq \gamma$.

It can be seen from Theorem 1 that if $\gamma > \gamma_{crit}$, then any trajectory that starts from the initial set $B_\psi(z_0, \gamma)$ will remain in the robustness ellipsoids $B_\psi(\xi(k; z_0, v), \gamma)$ in spite of input uncertainties bounded by δ (i.e. $\|\epsilon\|_\infty \leq \delta$). Therefore, we can apply the following piecewise linear feedback law $K_v(z)$ to guarantee safety:

$$K_v(z) \triangleq \begin{cases} \theta_1 z + \theta_{0,1}, & \text{when } z \in \mathcal{X}_1, \\ \theta_2 z + \theta_{0,2}, & \text{when } z \in \mathcal{X}_2, \\ \quad \vdots & \qquad \vdots \\ \theta_n z + \theta_{0,n_c}, & \text{when } z \in \mathcal{X}_{n_c}, \end{cases} \tag{11}$$

where $\{\mathcal{X}_i\}_{i=1}^{n_c}$ form a partition of the state space and the data points of the finitely many simulated trajectories in each partition $\mathcal{X}_i$ satisfy $|\theta_i z + \theta_{0,i} - v| < \delta$ (v is the optimal input of the feedforward controller corresponding to state z).

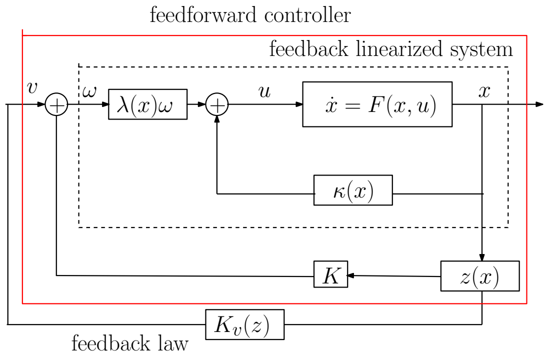

Fig. 1. Diagram of the feedforward and feedback controllers with the feedback linearized system.

We use ℓ to denote the index of the nominal (simulated) trajectories and we denote $\xi_\ell[k] \triangleq \xi_\ell(k; z_{0,\ell}, v_\ell)$. The clustering algorithm finds θ_i and $\theta_{0,i}$ that make the inequalities $|\theta_i \xi_\ell[k] + \theta_{0,i} - v_\ell[k]| < \delta$ true for as many k and ℓ as possible (Maximum Feasible Subsystem Problem), then remove those satisfied inequalities and repeat the same process over the remaining ones until all inequalities have been covered (for details, see [13]). The clusters are further split into subclusters (by k-means or other clustering methods) until the convex hull of each subcluster is disjoint with the convex hull of any other subcluster (otherwise the data points in different clusters may not be linearly separable and thus lead to loss of safety guarantee).

After all the disjoint subclusters are obtained, we classify all the subclusters using multi-class linear classification. There are two major approaches of multi-class linear classification: pairwise linear classifiers and piecewise linear classifiers. The pairwise linear classifiers classify each class with every other class and then use the intersection of all the half spaces determined by the pairwise decision boundaries as the partition for the class. It is easy to implement, but it is not guaranteed to form a complete partition of the whole state space (there may be "holes" that do not belong to any partition). The piecewise linear classifier can form a complete partition of the whole state space and therefore is a better fit for our approach. There are several different methods of constructing piecewise linear classifiers. One way is to construct n_c classification functions for the n_c subclasses such that at each data point the corresponding class function is maximal. We use robust linear programming to find the n_c classification functions for the n_c subclasses.

Definition 1 ([18]): For n_c sets $\mathcal{A}^i (i = 1, 2, \ldots, n_c)$ each consisting of m_c^i points in $\mathbb{R}^n$, represented by the $n \times m_c^i$ matrices A^i, are piecewise linear separable if there exists

$\omega^i, \omega^j \in \mathbb{R}^n$, $b^i, b^j \in \mathbb{R}$ such that

$$\omega^i A^i - e b^i > \omega^j A^i - e b^j, i, j = 1, 2, \ldots, n_c, i \neq j, \quad (12)$$

where e is a vector of ones.

The classification problem becomes the following linear programming (LP) problem:

$$\begin{aligned} \min. & \sum_{i=1}^{n_c} \sum_{j=1, j\neq i}^{n_c} \frac{e y^{ij}}{m_c^i}, \\ \text{s.t.} \ & y^{ij} \geq -(\omega^i - \omega^j) A^i + e(b^i - b^j) + e \\ & y^{ij} \geq 0, i, j = 1, 2, \ldots, n_c, i \neq j. \end{aligned} \quad (13)$$

We denote the resulting partition of the above LP optimization as $\{\hat{\mathcal{X}}_i\}_1^{n_c}$. We define the robustness ball as the smallest ball that covers the robustness ellipsoid. As a system state within one partition $\hat{\mathcal{X}}_i$ may not belong to any robustness ellipsoid within the partition $\hat{\mathcal{X}}_i$, but may belong to a robustness ellipsoid in another partition $\hat{\mathcal{X}}_j$ (for detailed illustration, see Fig. 4 of [12]), each partition is shrunk so that it does not intersect any robustness ball outside the partition and for each partition face, we make note of the robustness balls outside the partition that intersect it. Let $S_{ij} \triangleq \{(\ell, k) | -\left\|(\omega^i - \omega^j) P^{-\frac{1}{2}}\right\| \gamma_\ell < (\omega^i - \omega^j)\xi_\ell[k] + b^i - b^j < 0\}$ be the set of pairs (ℓ, k) where the robustness ball of the ℓth simulated trajectory at the kth time instant (outside of $\hat{\mathcal{X}}_i$) intersects the decision boundary between the ith and jth subcluster of data. We calculate $b_{ij}^- \triangleq \min_{(\ell,k)\in S_{ij}}(-\left\|(\omega^i - \omega^j) P^{-\frac{1}{2}}\right\| \gamma_\ell - (\omega^i - \omega^j)\xi_\ell[k])$, and thus obtain the new decision boundary $(\omega^i - \omega^j)x + b_{ij}^- = 0$. Thus we obtain a reduced partition $\mathcal{X}_i$ for each original partition $\hat{\mathcal{X}}_i$ such that a system state within $\mathcal{X}_i$ is guaranteed not to belong to a robustness ball in any other partitions.

When implemented online we use the following algorithm:
1) If the current state z lies within the reduced partition $\mathcal{X}_i$, use the feedback control law $K_v(z) = \theta_i z + \theta_{0,i}$;
2) If the current state lies within the original partition $\hat{\mathcal{X}}_i$, but not the reduced partition $\mathcal{X}_i$, check to see if it lies within any of the robustness balls marked in S_{ij} for the face that it lies near, then:
2a) If it does lie within a robustness ball centered at $\xi_\ell[k]$ and $\xi_\ell[k]$ lies within the jth partition ($j \neq i$), use the control law $K_v(z) = \theta_j z + \theta_{0,j}$;
2b) If it does not lie within any robustness ball, then still use the feedback control law $K_v(z) = \theta_i z + \theta_{0,i}$.

III. Energy Storage Controller Synthesis

In this section, we apply the controller synthesis method in designing an energy storage system (ESS) controller for regulating the grid frequency of a double-machine infinite-bus system as shown in Fig. 2 [19]. Two synchronous generators are denoted as G_i (i = 1, 2), while four constant impedance loads are denoted as L_j (j = 1, 2, 3, 4). The configuration parameters of the power system model and the line data can be seen in Tab. I and Tab. II. The swing dynamics of machine G_i (i = 1, 2) can be described by the following classical model:

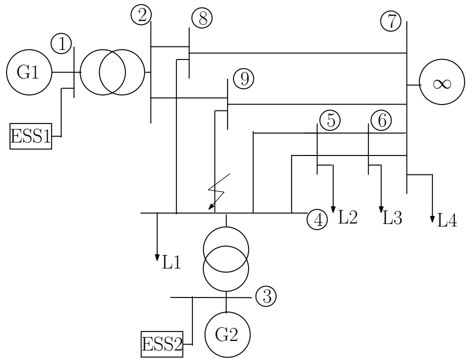

Fig. 2. Double-machine infinite-bus system.

$$\begin{cases} \dot{\delta}_i = \omega_i, \\ \frac{P_{ri}}{P_b} \frac{H_i}{\pi f_s} \dot{\omega}_i = P_{mi} - P_{ess_i} - D_i \omega_i - p_{ei}(\delta_1, \delta_2), \end{cases} \quad (14)$$

where δ_i is the rotor angle position of G_i with respect to the infinite bus at G_3, ω_i is the rotor speed deviation of G_i relative to system angular frequency $2\pi f_s$, P_b is the base power in the per unit system, P_{ri} is the rated power of G_i, H_i is the per-unit inertia constant, P_{mi} is the mechanical input power to G_i, D_i is the damping coefficient, P_{ess_i} is the power that flows from the grid to the energy storage system near G_i, the electrical output power P_{ei} is described by the following function of δ_1, δ_2 ($\delta_3 = 0$):

$$\begin{aligned} P_{ei}(\delta_1, \delta_2) \triangleq & G_{ii} V_i^2 + \sum_{j=1, j\neq i}^{3} V_i V_j \{G_{ij} \cos(\delta_i - \delta_j) \\ & + B_{ij} \sin(\delta_i - \delta_j)\}, \end{aligned} \quad (15)$$

where V_i is the voltage behind the transient reactance of G_i, G_{ii} is its internal conductance, $G_{ij} + jB_{ij}$ is the transfer admittance between G_i and G_j.

We use the following MTL specification for frequency regulation:

$$\begin{aligned} \phi = & \Box\neg\phi_1 \wedge \Box\neg\phi_2 \wedge \Box_{[2,T]}\phi_3, \\ \phi_1 = & (\omega_1 > 10), \phi_2 = (\omega_2 > 10), \\ \phi_3 = & (-2 \leq \omega_1 \leq 2) \wedge (-2 \leq \omega_2 \leq 2) \wedge (-\pi/2 \leq \delta_1 \leq \pi/2) \\ & \wedge (-\pi/2 \leq \delta_2 \leq \pi/2), \end{aligned}$$

which reads "The frequency deviations should never exceed 10 rad/s, after 2 seconds the frequency deviations should always be within ±2 rad/s and machine angles should always be within $\pm\pi/2$".

Assume that a three phase lines-to-ground fault occurs near bus 4 on line 4-9 and the resulting fault-on system

TABLE I

SYSTEM PARAMETERS

VA base P_b		160 MVA
System frequency f_s		60 Hz
Machine rating P_{ri} of G_i	i=1	82MVA
	i=2	160MVA
Mechanical input power P_{mi}	i=1	0.28 (pu)
	i=2	0.75 (pu)
Active power flow to load L_i	i=1	0.25 (pu)
	i=2	0.1875 (pu)
	i=3	0.4375 (pu)
	i=4	0.75 (pu)
Transient reactance of G_i	i=1	0.261 (pu)
	i=2	0.284 (pu)
Per-unit inertia constant H_i	i=1	5s
	i=2	3.5s
Damping coefficient D_i of G_i	i=1,2	0.01s
Voltage V_i of G_i	i=1,2	1.05 (pu)
Transformer impedance	G_1	1.8868 (pu)
	G_2	0.618 (pu)

TABLE II

LINE DATA (160MVA BASE)

Line number	Line impedance (pu)	Line charging (pu)
2-8(2-9)	0.0224+j0.1051	j0.0006625
7-8(7-9)	0.0880+j0.4080	j0.0023
4-8(4-9)	0.1168+j0.5440	j0.0031
4-5	0.0015+j0.0029	j0.0034
5-6	0.0023+j0.0032	j0.0094
6-7	0.0053+j0.0201	j0.0258

dynamics is as follows:

$$\begin{cases} \dot{x}_1 = & x_3; \\ \dot{x}_2 = & x_4; \\ \dot{x}_3 = & 74.3059(0.28 - 0.01x_3 - 1.05^2(0.0054985 \\ & -0.0031946\cos(x_1) + 0.22242\sin(x_1))); \\ \dot{x}_4 = & 53.8559(0.75 - 0.01x_4). \end{cases} \tag{16}$$

where the state $x = [\delta_1, \delta_2, \omega_1, \omega_2]^T$.

The post-fault system with the input $u = [P_{ess_1}, P_{ess_2}]^T$ is as follows:

$$\begin{cases} \dot{x}_1 = & x_3; \\ \dot{x}_2 = & x_4; \\ \dot{x}_3 = & 74.3059(0.28 - u_1 - 0.01x_3 - 1.05^2(0.006537+ \\ & 0.00089272\cos(x_1 - x_2) + 0.0027265\sin(x_1- \\ & x_2) - 0.0056368\cos(x_1) + 0.38079\sin(x_1)); \\ \dot{x}_4 = & 53.8559(0.75 - u_2 - 0.01x_4 - 1.05^2(0.00089272 \\ & \cos(x_2 - x_1) + 0.0027265\sin(x_2 - x_1)+ \\ & 0.010454 + 0.0077156\cos(x_2) + 1.0712\sin(x_2)). \end{cases} \tag{17}$$

As shown in Fig. 3, the post-fault system with no storage input ($u_1 = u_2 = 0$) is not stable as the second generator loses synchronism soon after the fault is cleared. Therefore a storage controller is necessary not only for the purpose of frequency regulation but also for maintaining the transient stability of the post-fault system.

We simulate 4 trajectories of the post-fault feedback linearized system (with the new input v to be optimized as described in Sec. II-B) starting from the fault-on trajectories cleared at 0.1912s, 0.1940s, 0.1967s and 0.1995s respectively. For the feedforward controller, we set $T = 10s$, $T_s = 0.1s$, $\zeta = 0.5$, (all the values are per unit values unless otherwise specified). As the optimization problem is not convex, we use the multi-start method to avoid getting stuck in local optimal solutions. The optimal storage input signals for the 4 different fault clearing time are shown in Fig. 4. It can be seen that in all 4 different scenarios, ESS 1 is hardly used while the power flows significantly from the grid to ESS 2 in the first 1 to 2 seconds to decrease the grid frequency. After this period, the power flow changes direction as the frequency deviation becomes negative and continues to decrease, so the storage has to generate electricity to prevent the frequency from dropping beyond the lower threshold. After the first 5 seconds, the storage control efforts gradually decrease to zero. It can also be seen that with longer fault clearing time, more (storage) control effort is needed to satisfy the MTL specification ϕ. The initial robustness ellipsoids of the simulated trajectory with fault clearing time of 0.1967s can totally cover the fault-on states with uncertainties in the fault clearing time (between 0.19s and 0.2s). Thus all the possible post-fault trajectories with the given uncertainties in the fault clearing time are guaranteed to satisfy the MTL specification ϕ (as shown in Fig. 5).

Next, we design a piecewise linear feedback law that is learned from the data of the simulated trajectory with fault clearing time of 0.1967s and the corresponding optimal inputs. We first cluster the 1001 data points into 84 disjoint subclusters while in each subcluster the input error is within δ=0.0118 (δ is designed such that $\gamma_{crit} < \min_{\ell} \gamma_\ell$). We generate the piecewise linear classifier to separate the 84 subclusters and modify the partitions according to the algorithm described in Sec. II-C. We generate 20 trajectories using the feedback controller over a sampling of initial conditions and demonstrate that the trajectories all satisfy the MTL specification ϕ (as shown in Fig. 6).

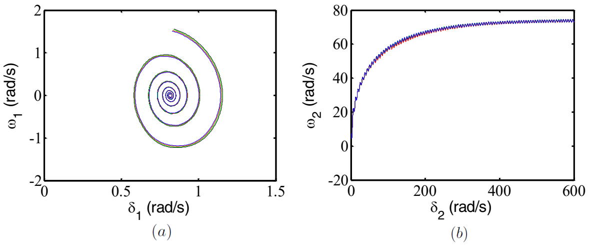

Fig. 3. 4 simulated trajectories of the post-fault system with no storage input over a sampling of initial conditions (fault clearing time between 0.19s and 0.2s).

IV. CONCLUSIONS

We presented an approach to optimally control the energy storage system for frequency regulation of power systems.

We use functional gradient descent method for the feedforward controller synthesis and the piecewise linear system identification techniques for the feedback controller synthesis. Both controllers can guarantee that all the post-fault trajectories with the given fault clearing time uncertainties satisfy the MTL specifications. The similar controller synthesis approach can be used in other related areas such as transient stability enhancement, voltage regulation, etc.

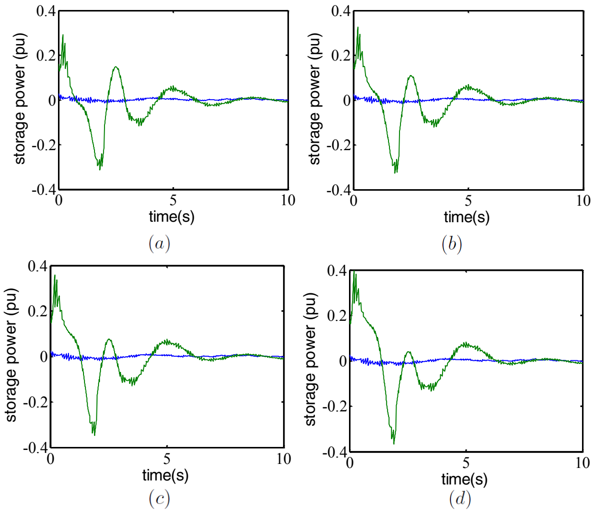

(a) (b) (c) (d)

Fig. 4. Storage input u (blue for ESS 1 and green for ESS 2) of the optimal feedforward controller with fault clearing time of (a) 0.1912s, (b) 0.1940s, (c) 0.1967s, (d) 0.1995s.

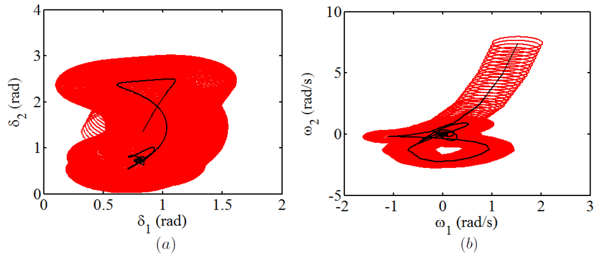

(a) (b)

Fig. 5. Robust neighbourhood of the nominal (simulated) trajectory of the post-fault feedback linearized system with the feedforward controller and the fault clearing time being 0.1967s.

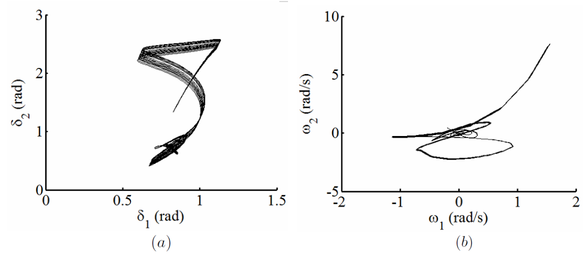

(a) (b)

Fig. 6. 20 trajectories generated by the feedback controller over a sampling of initial conditions (fault clearing time between 0.19s and 0.2s).

Acknowledgment

This research was partially supported by the National Science Foundation through grants CNS-1218109, CNS-1550029 and CNS-1618369.

References

[1] A. Mondal, S. Misra, and M. S. Obaidat, "Distributed home energy management system with storage in smart grid using game theory," *IEEE Systems Journal*, vol. PP, no. 99, pp. 1–10, 2015.

[2] Z. Xu, C. Belta, and A. A. Julius, "Temporal logic inference with prior information: An application to robot arm movements," *IFAC-PapersOnLine*, vol. 48, no. 27, pp. 141 – 146, 2015.

[3] Z. Xu and A. A. Julius, "Census signal temporal logic inference for multiagent group behavior analysis," *IEEE Trans. Autom. Sci. and Eng.*, 2016, in press. [Online]. Available: http://ieeexplore.ieee.org/document/7587357/

[4] Z. Xu, M. Birtwistle, C. Belta, and A. Julius, "A temporal logic inference approach for model discrimination," *IEEE Life Sciences Letters*, vol. 2, no. 3, pp. 19–22, Sept 2016.

[5] P. Tabuada, *Verification and Control of Hybrid Systems: A Symbolic Approach*. Springer US, 2009. [Online]. Available: https://books.google.com/books?id=1ExhrqtzIYwC

[6] E. M. Wolff, U. Topcu, and R. M. Murray, "Automaton-guided controller synthesis for nonlinear systems with temporal logic," in *Proc. IEEE/RSJ Int. Conf. Intell. Robots and Syst.*, Nov 2013, pp. 4332–4339.

[7] S. Coogan, E. A. Gol, M. Arcak, and C. Belta, "Traffic network control from temporal logic specifications," *IEEE Trans. Control of Network Systems*, vol. 3, no. 2, pp. 162–172, June 2016.

[8] A. Donze and V. Raman, "BluSTL: Controller synthesis from signal temporal logic specifications," in *ARCH14-15. 1st and 2nd International Workshop on Applied veRification for Continuous and Hybrid Systems*, ser. EPiC Series in Computing, G. Frehse and M. Althoff, Eds., vol. 34. EasyChair, 2015, pp. 160–168.

[9] S. Saha and A. A. Julius, "An MILP approach for real-time optimal controller synthesis with metric temporal logic specifications," in *Proc. IEEE Amer. Control Conf.*, July 2016, pp. 1105–1110.

[10] A. K. Winn and A. A. Julius, "Optimization of human generated trajectories for safety controller synthesis," in *Proc. IEEE Amer. Control Conf.*, June 2013, pp. 4374–4379.

[11] H. Abbas, A. Winn, G. Fainekos, and A. A. Julius, "Functional gradient descent method for metric temporal logic specifications," in *Proc. IEEE Amer. Control Conf.*, June 2014, pp. 2312–2317.

[12] A. K. Winn and A. A. Julius, "Feedback control law generation for safety controller synthesis," in *52nd IEEE Conference on Decision and Control*, Dec 2013, pp. 3912–3917.

[13] A. Bemporad, A. Garulli, S. Paoletti, and A. Vicino, "A bounded-error approach to piecewise affine system identification," *IEEE Trans. Autom. Control*, vol. 50, no. 10, pp. 1567–1580, Oct 2005.

[14] A. A. Julius and S. Afshari, "Using computer games for hybrid systems controller synthesis," in *49th IEEE Conference on Decision and Control (CDC)*, Dec 2010, pp. 5887–5892.

[15] G. E. Fainekos and G. J. Pappas, "Robustness of temporal logic specifications for continuous-time signals," *Theoretical Computer Science*, vol. 410, no. 42, pp. 4262 – 4291, 2009.

[16] H. Abbas and G. Fainekos, "Computing descent direction of MTL robustness for non-linear systems," in *Proc. IEEE Amer. Control Conf.*, June 2013, pp. 4405–4410.

[17] Y. Annpureddy, C. Liu, G. Fainekos, and S. Sankaranarayanan, *S-TaLiRo: A Tool for Temporal Logic Falsification for Hybrid Systems*. Berlin, Heidelberg: Springer Berlin Heidelberg, 2011, pp. 254–257.

[18] K. P. Bennett and O. L. Mangasarian, "Multicategory discrimination via linear programming," *Optimization Methods and Software*, vol. 3, pp. 27–39, 1992.

[19] Y. Susuki, T. Sakiyama, T. Ochi, T. Uemura, and T. Hikihara, "Verifying fault release control of power system via hybrid system reachability," in *Power Symposium, 2008. NAPS '08. 40th North American*, Sept 2008, pp. 1–6.